Retrofitting Potential of Building envelopes Based on Semantic Surface Models Derived From Point Clouds

Edina Selimovic[1], Florian Noichl[1], Kasimir Forth*[1], André Borrmann[1]

* Corresponding author, kasimir.forth@tum.de

1 Technical University Munich, Germany

Abstract

To meet the climate goals of the Paris agreement, the focus on energy efficiency needs to be shifted to increase the retrofitting rate of the existing building stock. Due to the lack of usable information on the existing building stock, reasoning about the retrofitting potential in early design stages is difficult. Therefore, deconstructing and building new is often regarded as the more reliable and economical option. Digital methods are missing or not robust enough to capture and reconstruct digital models of existing buildings efficiently and automatically derive reliable decision-support about whether demolition and new construction or retrofitting of existing buildings is more suitable. This paper proposes a robust, automated method for calculating existing buildings' life cycle assessments (LCA) using point clouds as input data. The main focus lies in bridging the gap between point clouds and importing semantic 3D models for LCA calculation. Therefore, the automation steps include a geometric transformation from point cloud to 3D surface model, followed by a semantic classification of the surfaces to thermal layers and their materials by assuming the surface elements by building age class.

Keywords

retrofitting potential, LCA, point cloud, semantic enrichment

DOI

https://doi.org/10.47982/jfde.2022.powerskin.8

1 INTRODUCTION

The construction sector is responsible for a large share of the overall situation of increasing emissions. In 2019, the amount of waste produced by the construction industry in Germany alone amounted to 230.9 million tons in 2019 (Umweltbundesamt, 2021). Most used materials are from non-renewable resources, mainly found in the existing building stock. At the same time, landfill capacities are decreasing and pose an additional environmental challenge to this industry sector (Hillebrandt, 2018; Rosen, 2018). Furthermore, the manufacturing, transportation, construction, and disposal of newly built assets, including buildings and infrastructure, contribute to 11% of the total carbon emissions worldwide (WorldGBC, 2019). For this reason, a particular emphasis is placed on the consideration of retrofitting instead of demolishing and building new. Consequently, retrofitting is regarded the most sustainable and ecologically most significant solution for the previously described problems in industrialized countries (Lottner, 2014; WorldGBC, 2019).
Due to the lack of usable information on the existing building stock, reasoning about the retrofitting potential in early design stages is difficult. Therefore, deconstructing and building new is often regarded as the more reliable and economical option (Matthias Hüttmann, 2018). Robust methods are missing to efficiently capture and reconstruct digital models of existing buildings (Deutscher Abbruchverband. 2007). The automatic derivation of reliable decision-support about whether demolition and new construction or retrofitting of existing buildings is more suitable is currently not supported (Matthias Hüttmann, 2018).

With the introduction of digital methods in the construction sector, such as Building Information Modeling (BIM), many conventional planning processes were facilitated (Borrmann, 2015). Synergies from many different disciplines have been identified, such as in the field of sustainability (BBSR & BBR, 2019). Since then, model-based sustainability analysis, for example, Life Cycle Assessment (LCA), can be realized in early design stages. However, previous research focused on pre-existing BIM models and neglected the existing building stock (Akbarieh et al., 2020).
The current way of creating a quantity take-off of an existing building is mostly a manual process, representing only an estimation and focused mainly on costs (Deutscher Abbruchverband, 2007). Remodeling would be highly time-consuming. To circumvent this, techniques have been developed in recent years that use digital methods to automatically generate 3D building models of a building through point cloud capture and processing. Automated processes for 3D Reconstruction and object recognition are therefore needed. These are yet not fully mature or applicable for the case of LCA calculation of existing buildings (Chen, 2021).
Addressing the mentioned problems, this paper proposes a method for bridging the gap between point clouds and importing semantic 3D models into tools for holistic calculation of the environmental impact of different scenarios. This research proves the opportunity to compare the environmental impacts and emissions between an existing building and a retrofitting variant and supports future decision-making without extensive manual preparation.

2 BACKGROUND AND RELATED WORK

This section discusses the background, related work, and the research gap for our proposed methodology. Firstly, we discuss the limitations of BIM in the end-of-life phases of building design. Secondly, we introduce the topic of geometric reconstruction of point clouds. In the end, we show approaches of object classification with a focus on windows as an exemplary addition and essential contribution to LCA calculations.

2.1 BIM IN THE END OF LIFE (EOL) DESIGN PHASE

Akbarieh et al. investigated the application of BIM in the EoL phase of buildings and to what extent BIM is used for planning in the EoL phase (Akbarieh et al., 2020). However, their research showed that most studies on BIM-based EoL topics were based on existing BIM models and did not investigate a simplified automated remodeling for different use cases. The applications developed mostly represent Application Programming Interfaces (APIs) for specific proprietary BIM tools in the form of Plug-Ins connected to LCA software. A direct data transfer between the 3D model and the LCA tool is often missing and not applicable without a workaround that includes specialized third-party software.

Studies conducted on existing buildings to investigate an EoL-related topic and therefore create a 3D model were carried out by Ge et al. (2017). They manually reconstructed the model with the help of plans, point clouds, and pictures, which is time-consuming. Volk et al. (2018) investigated an automatic approach that enabled the 3D reconstruction of the interior of a building based on a point cloud collected by a depth sensor. The building components were detected automatically, and the quantity take-off was calculated based on standard values and experience data to eventually perform a deconstruction analysis. Nevertheless, at some points, manual intervention was still needed.

2.2 3D RECONSTRUCTION

Employing digital surveying methods, existing buildings can be captured as point clouds. Reconstructing a 3D model from these point clouds has been a challenge in computer vision and computer graphics for years and is still an active field of research (Chen, 2021). The Poisson reconstruction by Kazhdan & Hoppe (2013) creates watertight surfaces from oriented point clouds. However, this approach requires complete data free of outliers, which is rarely the case for real-world measurements. Other papers address the problem of Manhattan-world scene reconstruction (Coughlan & Yuille 2000; Li et al., 2016), which represents the 3D scene with axis-aligned non-uniform boxes. Li et al.'s (2016) method successfully creates faithful reconstructions from various data sources. Still, this approach dramatically simplifies the geometric complexity of the real world. Nan & Wonka (2017) developed PolyFit, an approach that allows robust results for simple geometries with a slicing method. For this purpose, in a first step, the RANSAC algorithm (Schnabel et al., 2007) detects planes in the dataset. The next step clips the model with the detected planes in polyhedral cells, representing the candidates' faces. Described as an integer programming problem, the results of this approach are watertight and manifold. The only disadvantage lies in the scalability due to the extensive computation time needed for complex geometries (Nan & Wonka, 2017).

2.3 OBJECT CLASSIFICATION: WINDOW CLASSIFICATION

More semantic information can be added to create a model representation beyond the pure geometry of the building envelope. The window-to-wall ratio provides important information for energy simulation (Schneider & Coors, 2018). Therefore window classification is a suitable extension for a pure 3D reconstruction process.

There are many studies concerning window classification. Volk et al. use an image rendering of the point cloud walls to extract the windows (Volk et al., 2018). Yang et al. (2016). create a binary image to detect "holes" in the image Taraben & Kraemer (2021) use a deep learning approach to map the detected windows from 2D images on a previously generated surface model. Schneider & Coors (2018) recognize windows directly in the point cloud using a contouring algorithm.

Nevertheless, most studies treat windows as "holes" in the building hull and do not consider further features as radiometric properties. One advantage of point cloud acquisition by laser scanning is the ability to record intensity values. Intensity represents the amount of light reflected from a surface and is usually stored per point with a value from 0 to 255. It is assumed that each material can be approximated through a range of intensity values (Macher et al., 2021). The evaluation of intensity features is robust to light changes or shading but depends on scanner position, distance to object, and object colour (Macher et al., 2021; Park & Cho, 2021).
Park & Cho developed a deep learning method for material classification on 3D point clouds that consider intensity values in addition to geometric information and colour values (Park & Cho 2021). Macher et al. (2021) used intensity values to segment the windows from the facade based on a Histogram analysis. For this study, a laser scan point cloud should be used to investigate window classification based on intensity values.

3 METHODOLOGY

This section proposes a methodology for geometrically reconstructing surface models using point clouds as input, semantically enriching these models and importing them into an LCA tool. The acquisition of the point cloud derived from terrestrial laser scanning (TLS) is out of scope for this paper, as it is only used as the input for the proposed methodology. The geometric transformation from point cloud to 3D surface model is conducted using the PolyFit approach (Nan & Wonka, 2017). Transparent elements such as windows are identified through laser intensity values of the points. In the next step, the faces of the model can be assigned to thermal surface classes and finally imported into LCA software. The materials and material layers of the model faces are approximated by assuming the building age class. Figure 1 shows an overview of the workflow. The following subchapters introduce the steps of this workflow in more detail.

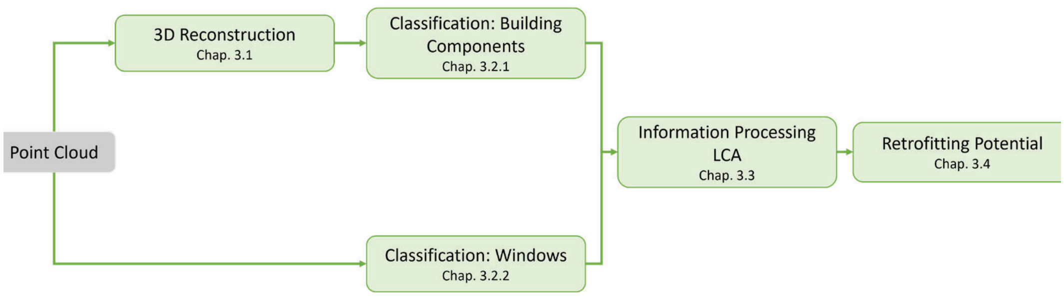

FIG. 1 The general workflow

3.1 3D RECONSTRUCTION

The process of creating the 3D shape and appearance of real objects is referred to as 3D reconstruction. In the following, the steps for reconstructing a 3D model out of a point cloud are explained in more detail. The entire methodology is shown in Figure 2.

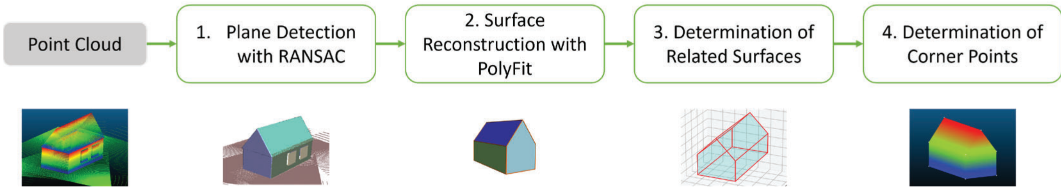

FIG. 2 Methodology for the 3D Reconstruction

To perform 3D reconstruction, the PolyFit approach is used. This approach is based on the RANSAC algorithm (Schnabel et al., 2007), which can identify planes from the point cloud. Thus, building surfaces, such as walls or roofs, can be captured individually. In PolyFit, the previously detected planes intersect with the point cloud's bounding box. This results in several faces, referred to as face candidates (Figure 3 - left). To determine the faces from the face candidates that form a common surface, PolyFit converts the reconstruction problem into a binary linear programming problem, resulting in the right picture of Figure 3.

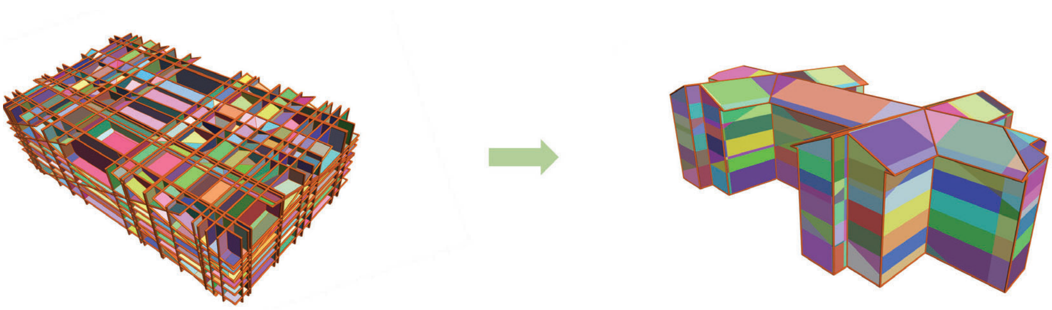

FIG. 3 PolyFit Result: Face Candidates (left) and selected face candidates (right)

The result can be exported as an OBJ-file (fileformat.info, 2022). The OBJ file contains information about all exterior surfaces and their corner points. The surfaces in the file represent the selected face candidates pictured on the right in Figure 3. However, for further applications, the combined building surfaces are more valuable. Hence, step 3 determines the combined surfaces formed by the selected face candidates. To identify them, this study uses the face normals. Face orientation can be determined using the dot product, starting from an XY-plane. In the last step the faces with the same normal orientation and at least one same point can be merged. After the related faces were detected, inner surfaces, in this case floors, are estimated using the building height. For this purpose, a floor height was assigned manually, which allowed the number of floors and their respective height coordinates to be estimated. The area of the floors is assumed to be identical to the ground floor.

Consequently, the corner points of the resulting surfaces are identified, as they are needed for further processing in LCA tools. Because the surface edges represent an intersection of straight lines, the condition can be set that corner points whose count is odd in the total set of points will represent a corner point of the total surface. This condition will take convex as well as concave polygonal surfaces into account. In this step, the order in the clockwise (CW) or counterclockwise (CCW) direction gets lost, and the corner points are listed in a random sequence. However, it is impossible to define a polygonal surface only by the point coordinates, so the order has to be rebuilt. To accomplish this, the point-edge relationships are considered beforehand. Consequently, the identified corner points can be ordered in a CW or CCW order.

3.2 OBJECT CLASSIFICATION

The surface model provides purely geometric information. To further use the model for LCA calculation, semantic information has to be added for a retrofitting potential analysis. In a first step, each surface is assigned to a thermal surface class, which will be later enriched with more material assumptions. In a second step, windows are classified to derive the window-to-wall ratios for the model.

3.2.1 Thermal Surface Classification

Each surface is assigned to a thermal class. The thermal surface classes describe the boundary conditions of each surface, e.g., wall to exterior or wall to the ground. There are 13 different classes existing (Hollberg et al., 2018). In this study, the following assumptions are made:

1. There is no basement floor
2. The flat and the pitched roof are referred to as the roof class
3. The walls considered only represent the walls to exterior
4. There is no distinction between ceilings
5. There is no distinction between windows in walls and roof windows

The thermal classes considered in this study can be classified based on simple geometric conditions, collected along with the thermal classes in Table 1. The basis for this classification is normalized surface normal vectors, rounded to one decimal. The classes are determined through the surfaces' orientation to the XY-plane, where rounding to one decimal leads to a tolerance of 2.8° for single-axis rotation and 4.0° rotation around two axes.

TABLE 1 **Thermal Surface Classification**

Thermal surface class	Condition 01	Condition 02
Floor to Ground	Orientation parallel to XY-plane	Lowest z-coordinates
Flat Roof	Orientation parallel to XY-plane	Not the Floor surface
Pitched Roof	Orientation neither parallel nor perpendicular to XY-plane	
External-Wall	Orientation perpendicular to XY-plane	
Ceiling	Assumed floor height and floor number, dependent on total building height	Orientation parallel to XY-plane and equally shaped as the floor to ground

3.2.2 Window Classification

The window classification is carried out using intensity values. These are obtained from the laser scan and stored with the points in the point cloud. Therefore, the window classification is performed directly on the point cloud in contrast to the thermal surface classification. For the LCA calculation, the window-to-wall ratio was estimated. An accurate geometric representation was not needed. Figure 4 shows a summary of the classification process.

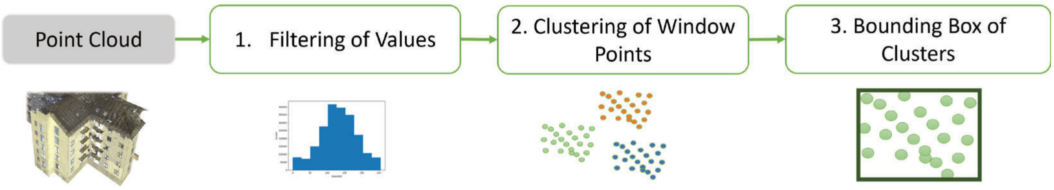

FIG. 4 Process for the Window Classification

In this study, the window points are extracted by their intensity values. Therefore, the values of the whole point cloud are analyzed in a histogram. Hence giving an initial range for the façade values, from which the range of values for the windows can be approximated. The range must be adjusted specifically to the project and is refined within the case study (Chapter 4.3). The range with the most window points and the fewest false points is iteratively filtered out. False points refer to points whose intensity values overlap with the window points. To define a clear assignment of points to each window, the points defining one window are clustered into a group, which is necessary to extract the windows individually. The window points are clustered with the density-based DBSCAN-Clustering by Ester et al., (1996). The algorithm depends on the parameter eps, which describes the minimal radius that combines all points within this radius to a cluster. A weakness of the intensity-based approach is that the window points are not fully captured in the point cloud processing due to the transparent material property of glass, which leads to an inaccuracy in the detected clusters and thus only represents an approximation. Consequently, the bounding boxes around the clusters, determined in the last step, were not perfectly rectangular.

3.3 INFORMATION REQUIREMENT AND PROCESSING FOR THE LCA

Certain information is required to perform an LCA from a semantic enriched 3D model. The information can be represented in alphanumerical numbers, coordinates, etc., and is needed for different reasons within the LCA calculation. Table 2 gives an overview of the required types of information.

TABLE 2 **LCA required Input Information**

Information	In the form of	Usage for LCA calculation
Surfaces	XYZ-coordinates of the corner points	Essential for whole LCA
Area of the surface	Alphanumerical number	Essential for whole LCA
Surface material	By assumption of the surface elements by building age class	Essential for whole LCA
Thermal Layer of the surface	Text label	Calculation of the use phase
Outward-facing surface normal	Vector	Calculation of the use phase
Window openings in surface	Number of the surface area and ID of the window	Essential for whole LCA Window-to-wall ratio

The surface area of the polygonal surfaces and windows is calculated based on the corner point coordinates. Therefore, the surface is split into triangles, which allows taking convex as well as concave surfaces into account. The area can be calculated using the cross product of each triangle. The sum of all triangle areas determines the total area. Afterwards, the window-to-wall ratio is calculated by dividing the previously classified window area by the total area. In the last step, the outward-facing normal of every surface is defined, needed to calculate the use phase in the LCA.

This computation represents a common problem, which is solved with the Trimesh library (Dawson-Haggerty et al. 2019) and is not applicable for objects with high geometric complexity.
As a final step, in the LCA calculation tool, the material layers and material thicknesses of the model faces are approximated by assuming the building age class. Therefore, the information from the TABULA database is combined with the LCA database using OEKOBAUDAT (BBSR 2022).

3.4 CALCULATION OF THE RETROFITTING POTENTIAL

The calculated retrofitting potential in this study aims to compare the environmental impacts of the existing building with a retrofitting variant using LCA. To simplify and enable the comparability of the variants, the following assumptions as well as system boundaries and boundary conditions were made:

- No consideration of the lifecycle phase C for the demolition of reconstructed old substances according to the Rating System Sustainable Building (BMUB, 2017)
- Considered useful lifespan of the building: 50 years
- Chosen environmental indicators: primary energy non-renewable and global warming potential (GWP)
- Manual specification of an identical energy system

In summary, the retrofitting potential will compare only newly installed materials in all lifecycle phases. A detailed analysis for recycling and demolitions efforts of existing building components is out of scope, as in this early design phase, no reliable assumptions can be made.

4 CASE STUDY

4.1 DATASET AND PREPROCESSING

To test and validate the proposed method, this study conducted a case study on a point cloud (see Figure 5.a) obtained by a TLS of an existing 5-storey multi-apartment building from the 1960s (MERKO 2022). The point cloud of the abandoned building, situated in Adazi, Latvia, was acquired due to the building's need for retrofitting. First of all, the point cloud with 10.315.268 points was subsampled within the open source software CloudCompare (CloudCompare 2022) through the specification of space between the points to 0.1 m. In the used point cloud, the points of the interior of the building were also contained. To simplify computation, these points were removed manually. To reconstruct the 3D model, the planes were detected with the RANSAC algorithm (see Figure 5.b) and the surface model was generated using the PolyFit software. Here the complexity was reduced with the provided PolyFit parameters, allowing simplified further processing. The obtained surface model consisted of selected face candidates from PolyFit (see Figure 3 right). In the next step, related faces were combined with building surfaces (see Figure 5.c), allowing the extraction of the corner points' coordinates.

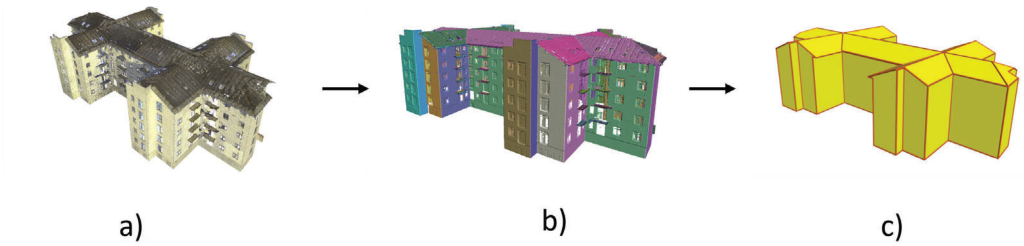

FIG. 5 a) The Point Cloud with b) the Detected Planes from RANSAC and c) the Reconstructed Surface Model from PolyFit

4.2 SEMANTIC ENRICHMENT AND WINDOW CLASSIFICATION

Subsequent steps deal with semantic enrichment. Thermal surface classification is conducted on the geometric surface model. Due to simplified assumptions, the implemented classification system classified all walls as exterior walls and the floor as floor-to-ground. A building with a cellar is not considered here. Furthermore, the ceiling structure is always the same, and there is no ceiling against unheated space. In addition, recesses in the ceilings cannot be taken into account. Extensions or garages with flat roofs are excluded since only one roof is assumed.
The windows were detected separately in the point cloud file, providing the laser intensity information. After the performed Histogram analysis of intensity values, it was observed that the intensity values of window elements were heavily spreading. Nevertheless, almost all window intensity points lay in a range from 0 to 40, with some outliers at value 255. In between, there were virtually no window points detected. However, choosing all points in a range [0;40] would lead to many false points, mainly from the roof and the building edges (see Figure 6.b). This is most likely the case due to standard sensitivity factors of laser scanners, such as the scanner position, the incidence angle, and the distance to the acquired object. The determination of the window range is thus project-specific, and a range of [0;25] was iteratively set as the most accurate for this point cloud.

On this basis, the window points were extracted, and the DB-Scan Clustering was performed to further extract the windows individually (see Figure 6.c). Here the parameter describing the minimal distance of a point to a cluster was set to 0.4 m. This value is set to prevent nearby window points from being merged into one cluster. The clustering results still showed that some windows were merged, but on the downside, some were neglected totally. Nevertheless, this was largely compensated in the overall results.
Due to the intensity-based approach, some false points that were not describing windows, but overlapping in intensity values, were extracted too. This led to falsely detected clusters from these points. Some were removed based on their orientation parallel to the XY-plane, as they were representing balconies. Others were removed based on their very low height, which is not common for windows, thus representing the lower building edge.

In the last step, the bounding boxes were defined around each cluster (see Figure 6.d). Due to some missing window points, the boxes were not perfectly rectangular but also rhomboid-shaped. This was acceptable since only the ratio is to be examined, and the geometrical form of the recognized windows is of secondary importance. Consequently, the corner points were determined and the area calculated. The results showed a detection rate of approximately 94 %, with a total window area of 1129.62 m^2 compared to the correct area of around 1200 m^2.

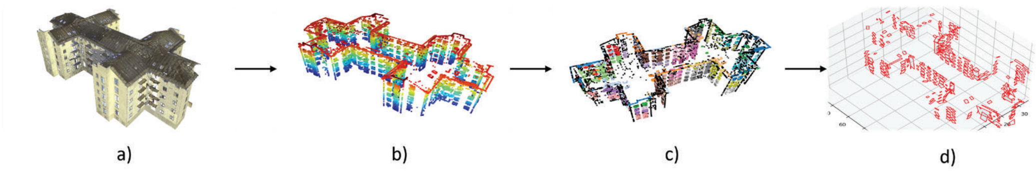

FIG. 6 a) point cloud with b) filtered window points and c) clustered windows, and d) cluster-fitted bounding boxes

4.3 LCA CALCULATION OF RETROFITTING POTENTIAL

Subsequently, the gained information was processed as input in an LCA tool. Due to its LCA-based direct variant comparison function, the LCA software used in this study was CAALA (CAALA 2020). Moreover, CAALA enables the calculation of the total emissions, embodied and operational energy, using a single-zone calculation approach. For this purpose, the data was converted into a CAALA-JSON file. Therefore, the area, the surface outward normal, and the window-to-wall ratio was calculated, as described in Chapter 2.3.
After the geometry was read in the software, the material layers were assumed by building age class. The investigated building complex was assumed to be building type NBL_MFH_E (1958-1968) according to the TABULA building type defined by the institute for housing and environment in the course of an EU project (Loga et al., 2015).
In the next step, the retrofitting variant was developed considering the building age, including the following measures, which CAALA suggests for this construction:

1. Wood fibre insulations in an external thermal insulation composite system (ETICS)
2. Triple glazing windows with a wooden frame, U=0.8, g=0.6
3. the energy system of a condensing gas boiler

The refurbished variant leads to much better results regarding energy performance as well as greenhouse gas emissions. This is represented in Table 3 with the total non-renewable primary energy consumption (PENRT) and the greenhouse gas emissions (GWP) of the existing building in comparison to the emissions of the refurbished variant. All lifecycle phases were considered for the calculation as described in Section 3.4.
Furthermore, Figure 7 depicts the cumulative emissions of the GWP over the whole lifecycle. Here the existing building starts with no emissions and finishes the first year with 78.53 kg CO_2-eq./(m^2NGF*a) from the building's operational phase B6. The retrofitted variant starts with -24.0 kg CO_2-eq./(m^2NGF*a) resulting from phases A1-3 due to sustainable materials used and increases annually by 26.56 kg CO_2-eq./(m^2NGF*a) on account of the operational phase B6. In contrast to the retrofitted variant, the emissions from the end of life phase C of the existing building are not considered as described by the considered systematic of the sustainable rating system (BMUB, 2017). This can be seen in Figure 7 from the different incline at the end of the two graphs.Only simple retrofitting measures were chosen to validate the workflow, as the focus is on the automated generation of geometric and semantic information rather than on different and complex retrofitting scenarios.

TABLE 3 **LCA results of the variant comparison**

LCA indicator	Unit	Existing Building	Retrofitted variant
Primary energy non-renewable (PENRT)	[kWh/(m^2NGF*a)]	358.74	129.14
Global Warming Potential (GWP)	[kg CO_2-eq./(m^2NGF*a)]	78.53	28.43

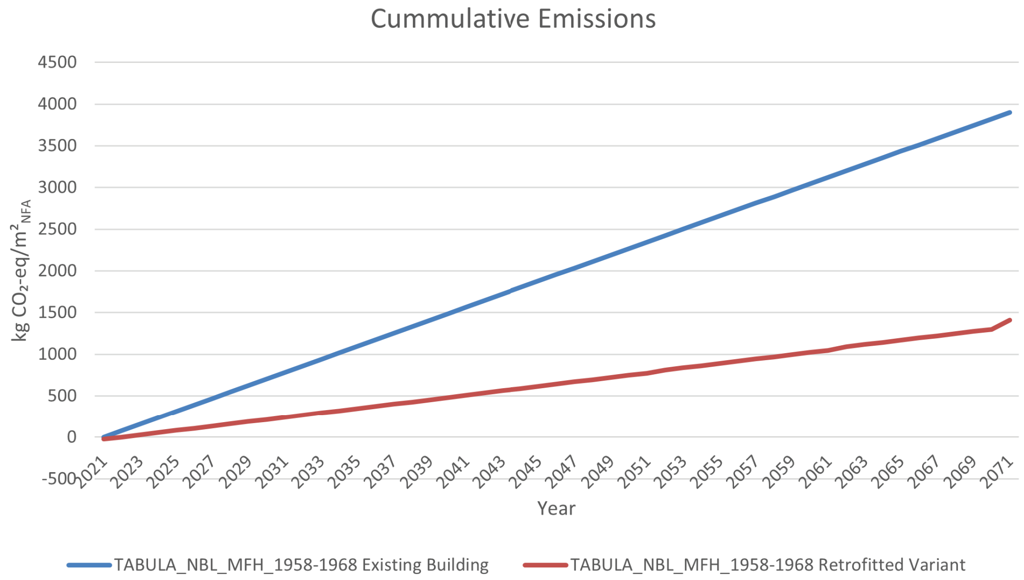

FIG. 7 Cumulative Emissions of the GWP of the Compared Variants

5 DISCUSSION

The proposed method enables LCA calculation of retrofitting scenarios on the basis of semantic 3D models generated and enriched from point clouds. The method was tested on a 5-storey multi-apartment building. The study verified that a point cloud of the building's envelope could be processed in such a way that the minimum geometric and semantic requirements needed for an LCA calculation and the import into an LCA tool can be obtained. The proposed methodology leads to widening the scope of action for construction decisions on retrofitting the existing building stock already in early design stages. Moreover, the ability of semantic enrichment of 3D models with intensity values for window classification was demonstrated.

Limitations of the developed method can be faced if the geometric complexity is too high, resulting in an inaccurate surface model or a wrong surface outward normal computation. The latter would lead to an incorrect LCA calculation of the use phase and, therefore, only enable the calculation of the embodied energy, which is insufficient for the making of a meaningful decision.

Furthermore, the classification of the windows requires manual adjustment for filtering the intensity values of the window points. The investigation of laser intensity values restricts the digital surveying technology to laser scanning and the results to the quality of the acquired window points. It has to be mentioned that the results of the window classification represent a window-to-wall ratio and not an accurate geometric shape, which is, however, sufficient for a simplified LCA calculation in an early design phase.

The LCA results strongly depend on the selected materials and thicknesses and on the assumptions of the TABULA building typology. Furthermore, the material allocation is not performed independently but requires this function in the software.

6 CONCLUSION AND OUTLOOK

Regarding the building sector's climate goals and environmental impacts, the retrofitting rate needs to be increased instead of the number of new constructions. Hence, this paper proposes an automated method to calculate the LCA of existing buildings by using point clouds as input data to close the gap between point clouds and LCA software. To validate the method, a point cloud acquired with a laser scanner of an existing building was used, containing the intensity values of each point. The geometrical reconstruction was conducted using the PolyFit approach. The semantic enrichment of the building components was based on geometrical information, while the windows were classified using intensity values. For this study, the window-to-wall ratio was sufficient. Thus, the geometric representation of the windows was not needed. The developed method detected around 94 % of the total window area and mapped the windows to the appropriate walls.

In future works, the importance of 3D reconstruction, and similarly, Scan-to-BIM processes, will increase, opening up a wide synergy potential for many research fields, such as sustainability. Furthermore, radiometric features such as intensity should be investigated in future studies, especially in the promising field of deep learning. The consideration of intensity values could enable a material classification from the point cloud and therefore help to identify more information about surface materials. This could lead to a direct assumption of building classes. Besides, the window classification can be more sensitized to determine the geometric shape. Thus, a combination of the usage of intensity values with a deep learning technology could lead to promising results.

References

Akbarieh, A., Jayasinghe, L. B., Waldmann, D., & Teferle, F. N. (2020). BIM-Based End-of-Lifecycle Decision Making and Digital Deconstruction: Literature Review. *Sustainability*, *12*(7), 2670. https://doi.org/10.3390/su12072670

BBSR, & BBR (2019). *Ökobilanzierung und BIM im Nachhaltigen Bauen [Life Cycle Assessment and BIM in Sustainable Construction]*. Retrieved from https://www.bbsr.bund.de/BBSR/DE/forschung/programme/zb/Auftragsforschung/2NachhaltigesBauenBauqualitaet/2019/oekobilanz-bim/01-start.html

BBSR, Ö. (2022, May 20). ÖKOBAUDAT. Retrieved from https://www.oekobaudat.de/en.html

BMUB (2017). *Bewertungssystem Nachhaltiges Bauen (BNB). Büro- und Verwatungsgebäude. Modul Komplettmodernisierung. BNB_BK 1.1.1: Ökologische Qualität. Wirkungen auf die globale und lokale Umwelt. Treibhausgaspotential (GWP) [Sustainable Building Rating System (BNB). Office and administration buildings. Module whole-building modernization. BNB_BK 1.1.1: Environmental quality. Effects on the global and local environment. Greenhouse gas potential (GWP)]*. Retrieved from https://www.bnb-nachhaltigesbauen.de/bewertungssystem/buerogebaeude/steckbriefe-bnb-bk-2017/

Borrmann, A. (2015). *Building Information Modeling: Technologische Grundlagen und Industrielle Praxis [Building Information Modeling: Technological Basics and Industrial Practice]. VDI-Buch Ser*. Wiesbaden: Springer Fachmedien Wiesbaden GmbH. Retrieved from https://ebookcentral.proquest.com/lib/kxp/detail.action?docID=3567925

CAALA (2020, August 3). Ihr digitaler Assistent für ganzheitliches Entwerfen. – CAALA [Your digital assistant for holistic design. – CAALA]. Retrieved from https://caala.de/

Chen, Z. (2021). *Learning to Reconstruct Compact Building Models from Point Clouds* (Master Thesis). Delft University of Technology. Retrieved from https://repository.tudelft.nl/islandora/object/uuid:e33e7fa1-118e-41d8-904f-5f03eb36e887?collection=education

CloudCompare (2022). CloudComapre (Version 2.12.1) [Computer software]. CloudCompare: CloudCompare. Retrieved from http://www.cloudcompare.org/

Coughlan, J. M., & Yuille, A. L. (2000). *The Manhattan World Assumption: Regularities in scene statistics which enable Bayesian inference.*

Dawson-Haggerty et al. (2019). Trimesh (Version 3.2.0) [Computer software]. Retrieved from https://trimsh.org/

Abbrucharbeiten: Grundlagen, Vorbereitung, Durchführung [Demolition work: Fundamentals, preparation, execution]. (2., aktualisierte und erw. Aufl.) (2007). Köln: R. Müller.

Fileformat.info (2022, May 11). Wavefront OBJ: Summary from the Encyclopedia of Graphics File Formats. Retrieved from https://www.fileformat.info/format/wavefrontobj/egff.htm

Ge, X. J., Livesey, P., Wang, J., Huang, S., He, X., & Zhang, C. (2017). Deconstruction waste management through 3d reconstruction and bim: A case study. *Visualization in Engineering*, *5*(1), 1–15. https://doi.org/10.1186/s40327-017-0050-5

Hollberg, A., Lichtenheld, T., Klüber, N., & Ruth, J. (2018). Parametric real-time energy analysis in early design stages: A method for residential buildings in Germany. *Energy, Ecology and Environment*, *3*(1), 13–23. https://doi.org/10.1007/s40974-017-0056-9

Kazhdan, M., & Hoppe, H. (2013). Screened poisson surface reconstruction. *ACM Transactions on Graphics*, *32*(3), 1–13. https://doi.org/10.1145/2487228.2487237

Li, M., Wonka, P., & Nan, L. (2016). Manhattan-World Urban Reconstruction from Point Clouds. In (pp. 54–69). Springer, Cham. https://doi.org/10.1007/978-3-319-46493-0_4

Loga, T., Diefenbach, N., & Born, R. (2015). *Deutsche Gebäudetypologie: Beispielhafte Maßnahmen zur Verbesserung der Energieeffizienz von typischen Wohngebäuden [German building typology: Exemplary measures for improving the energy efficiency of typical residential buildings]*. Darmstadt.

Macher, H., Roy, L., & Landes, T. (2021). Automation of windows detection from geometric and radiometric information of point clouds in a scan-to-BIM process. *The International Archives of the Photogrammetry, Remote Sensing and Spatial Information Sciences*, *XLIII-B2-2021*, 193–200. https://doi.org/10.5194/isprs-archives-XLIII-B2-2021-193-2021

Matthias Hüttmann (2018). *Graue Energie Abreißen oder sanieren? [Demolishing or retrofitting embodied energy?]* BUND-Jahrbuch 2018 Ökologisch Bauen Und Renovieren: Nachhaltige Orientierung f*ür Bauherren*, 16–19. Retrieved from chrome-extension://efaidnbmnnnibpcajpcglclefindmkaj/viewer.html?pdfurl=https%3A%2F%2Fwww.bund-bawue.de%2Ffileadmin%2Fbawue%2FDokumente%2FThemen%2FKlima_und_Energie%2FOEkologisch_Bauen_und_Renovieren_2018_Graue_Energie._Abreissen_oder_sanieren.pdf&clen=913329&chunk=true

MERKO (2022, May 11). DEMO DATA | Drupal. Retrieved from http://www.merko.lv/en/demo-data

Nan, L., & Wonka, P. (2017). *PolyFit: Polygonal Surface Reconstruction from Point Clouds*. https://doi.org/10.1109/ICCV.2017.258

Park, J., & Cho, Y. K. (Eds.) (2021). *Laser Intensity-assisted Construction Material Classification in Point Cloud Data using Deep Learning*. Orlando, FL.

Schnabel, R., Wahl, R., & Klein, R. (2007). Efficient RANSAC for Point-Cloud Shape Detection. *Computer Graphics Forum*, *26*(2), 214–226. https://doi.org/10.1111/j.1467-8659.2007.01016.x

Schneider, S., & Coors, V. (2018). *Automatische Extraktion von Fenstern in 3D Punktwolkenmittels einer hierarchischen Methode [Automatic extraction of windows in 3D point clouds using a hierarchical method]* (38. Wissenschaftlich-Technische Jahrestagung der DGPF und PFGK18 Tagung in München No. 27). München. Retrieved from https://www.researchgate.net/publication/323749844_Automatische_Extraktion_von_Fenstern_in_3D_Punktwolken_mittels_einer_hierarchischen_Methode

Taraben, J., & Kraemer, K. (2021). *Automatisierte Generierung von Stadtmodellen aus UAS-Befliegungen für die energetische Bewertung von Quartieren [Automated generation of city models from UAS flights for the energetic evaluation of neighborhoods]* (32. Forum Bauinformatik 2021).

Umweltbundesamt (2021, November 29). Abfallaufkommen [Volume of Waste]. Retrieved from https://www.umweltbundesamt.de/daten/ressourcen-abfall/abfallaufkommen#bau-abbruch-gewerbe-und-bergbauabfalle

Volk, R., Luu, T. H., Mueller-Roemer, J. S., Sevilmis, N., & Schultmann, F. (2018). Deconstruction project planning of existing buildings based on automated acquisition and reconstruction of building information. *Automation in Construction*, *91*, 226–245. https://doi.org/10.1016/j.autcon.2018.03.017

Yang, J., Shi, Z.-K., & Wu, Z.-Y. (2016). Towards automatic generation of as-built BIM: 3D building facade modeling and material recognition from images. *International Journal of Automation and Computing*, *13*(4), 338–349. https://doi.org/10.1007/s11633-016-0965-7